Journal of Thermal Biology 112 (2023) 103467

Contents lists available at ScienceDirect

Journal of Thermal Biology

journal homepage: www.elsevier.com/locate/jtherbio

Assessment of chronic limb threatening ischemia using thermal imaging

Tomppa Pakarinen [a,*], Atte Joutsen [c], Niku Oksala [a,b], Antti Vehkaoja [a]

[a] Faculty of Medicine and Health Technology, Tampere University, Postal: Tampereen Yliopisto, Korkeakoulunkatu 3, 33720, Tampere, Finland
[b] Vascular Surgery and Procedural Radiology, Tampere University Hospital, Postal: Elämänaukio 2, 33520, Tampere, Finland
[c] Department of Medical Physics, Medical Imaging Center, Tampere University Hospital, Postal: Sädetie 6, 33520, Tampere, Finland

ARTICLE INFO

Keywords:
Peripheral artery disease
Chronic limb threatening ischemia
Thermal imaging
Blood perfusion
Dynamic imaging

ABSTRACT

Objectives: Current chronic limb threatening ischemia (CLTI) diagnostics require expensive equipment, using ionizing radiation or contrast agents, or summative surrogate methods lacking in spatial information. Our aim is to develop and improve contactless, non-ionizing and cost-effective diagnostic methods for CLTI assessment with high spatial accuracy by utilizing dynamic thermal imaging and the angiosome concept.

Approach: Dynamic thermal imaging test protocol was suggested and implemented with a number of computational parameters. Pilot data was measured from 3 healthy young subjects, 4 peripheral artery disease (PAD) patients and 4 CLTI patients. The protocol consists of clinical reference measurements, including ankle- and toe-brachial indices (ABI, TBI), and a modified patient bed for hydrostatic and thermal modulation tests. The data was analyzed using bivariate correlation.

Results: The thermal recovery time constant was on average higher for the PAD (88%) and CLTI (83%) groups with respect to the healthy young subjects. The contralateral symmetry was high for the healthy young group and low for the CLTI group. The recovery time constants showed high negative correlation to TBI ($\rho = -0.73$) and ABI ($\rho = -0.60$). The relation of these clinical parameters to the hydrostatic response and absolute temperatures ($|\rho| < 0.3$) remained unclear.

Conclusion: The lack of correlation for absolute temperatures or their contralateral differences with the clinical status, ABI and TBI disputes their use in CLTI diagnostics. Thermal modulation tests tend to augment the signs of thermoregulation deficiencies and accordingly high correlations were found with all reference metrics. The method is promising for establishing the connection between impaired perfusion and thermography. The hydrostatic modulation test requires more research with stricter test conditions.

1. Introduction

Chronic Limb Threatening Ischemia (CLTI) is a condition that may at its worst lead to necrosis, blood poisoning, and finally amputation of the limb or even death if untreated. Lower limb blood perfusion i.e., the delivery of oxygenated blood and nutrients to the tissues can be permanently disturbed due to certain medical conditions, the most important of which is peripheral arterial disease (PAD) caused by atherosclerotic narrowings, leading to significant pressure loss along the arterial tree, resulting in impaired blood perfusion and subsequently in ischemia.

Current diagnosis of different forms of PAD are based on clinical examination, physiological measurements such as Ankle-Brachial-index (ABI), toe-brachial index (TBI), toe systolic pressure, transcutaneous oximetry, or skin perfusion pressure (SPP) and imaging (Gerhard-Herman et al., 2016; Misra et al., 2019). These methods have severe limitations: varying diagnostic accuracy, bias due to media sclerosis, invasiveness, and sensors requiring contact with the patient and lack of spatial information on perfusion and no information on all factors needed to estimate the sufficiency of perfusion (Misra et al., 2019; Xu et al., 2010; Tehan et al., 2016). There is a real need to develop methods overcoming the current diagnostic limitations, and techniques that could guide the treatment procedures by providing real time information on the spatial perfusion of the lower limb.

Thermal imaging (TI) is a contactless imaging modality, which is used to detect thermal radiation, naturally emitted by any object above absolute zero. Modern thermal cameras can acquire 2-dimensional

Abbreviations: Chronic Limb Ischemia (CLTI), Peripheral Artery Disease (PAD); Toe-Brachial Index (TBI), Ankle-Brachial Index (ABI).

* Corresponding author.
E-mail addresses: tomppa.pakarinen@tuni.fi (T. Pakarinen), atte.joutsen@pshp.fi (A. Joutsen), niku.oksala@pshp.fi (N. Oksala), antti.vehkaoja@tuni.fi (A. Vehkaoja).

https://doi.org/10.1016/j.jtherbio.2023.103467
Received 3 August 2022; Received in revised form 20 December 2022; Accepted 22 December 2022
Available online 12 January 2023

Nomenclature

g	Gravitational acceleration (ms^{-2})
ϱ	Fluid density ($kg \bullet m^{-3}$)
l	Limb length measured from the greater trochanter (m)
Δp	Change in hydrostatic pressure ($kg \bullet ms^{-2}$)
θ_{elev}	Limb elevation angle ($^{\circ}$ deg)
t	Time (s)
T_0	Initial temperature ($^{\circ}C$)
$T(t)$	Temperature with respect to time ($^{\circ}C$)
τ	Time constant (s)
A	Thermal recovery scaling constant ($^{\circ}C/s$)
ρ	Pearson rho correlation coefficient
r_s	Spearman rho correlation coefficient
T_{rel}	Relative temperature difference between rest and limb elevation ($^{\circ}C$)
T_{rest}	Mean region of interest temperature during the rest period ($^{\circ}C$)
T_{elev}	Mean region of interest temperature during the limb elevation period ($^{\circ}C$)
T_{recov}	Mean region of interest temperature during recovery period ($^{\circ}C$)

thermal data in high resolution and frame rate, detecting temperature changes in range of 10 mK. TI has been previously utilized in different fields of medicine, such as to detect breast cancer (Mambou et al., 2018), to study inflammatory diseases and sport injuries (Ring and Ammer, 2012; Bharara et al., 2006) and to diagnose circulatory conditions (Bagavathiappan et al., 2009; Ring and Ammer, 2012). Research on the suitability of the TI-based perfusion estimation in diabetic patients has been intensive (Peregrina-Barreto et al., 2014; Mori et al., 2013; Gatt et al., 2018; Bagavathiappan et al., 2010). For diabetic patients, the results have been promising showing changes in lower limb temperature profiles and asymmetries in diabetic feet (Gatt et al., 2018), as well as connection between thermal hot spots and elevated risk of ulceration (Gatt et al., 2015; Bagavathiappan et al., 2009). A statistically significant correlation between the post-PTA lower limb perfusion and ABI has been found (Misra et al., 2019), but the link between thermography and true perfusion remains unclear and full potential of TI in different phases of clinical pathway requires further studies including standardized measurement protocols and analysis methods (Staffa et al., 2017). Additionally, majority of the previous research focuses solely on the static acquisition and absolute measures, thus omitting dynamic body processes and the possibility of modulation tests. The potential advantages and methods in dynamic TI have been investigated previously (Kaczmarek and Nowakowski, 2016; Soliz et al., 2016; Sagaidachnyi et al., 2016; Geyer et al., 2004), but the connection to clinical diagnostic parameters for CLTI has not been established.

In this paper, we suggest and test a methodology for dynamic lower limb thermography using thermal and hydrostatic modulation in combination with the angiosome concept, where the lower limb is divided in single source artery supplied regions. Our aim is to develop non-contact and non-invasive methods for assessing the vascular condition and diagnosing chronic limb threatening ischemia, which could possibly be extended to real-time monitoring during the treatment and post-treatment surveillance. The combination of the modulation tests and dynamic TI with the angiosome concept is a novel approach in determining the connection between TI, PAD severity and CLTI.

2. Methods

2.1. Patients

The study has obtained favorable statement from the ethics committee of Tampere University Hospital (R19075L) and has been approved by the Nation Competent Authority, FIMEA (2020/001201). Data was collected at Tampere University hospital at vascular surgery and operative radiology unit (VETO) during August 2021. Data consists of 3 healthy young volunteers with no history of cardiovascular disease, 4 patients with PAD with claudication and 4 volunteering patients diagnosed with CLTI. The data was considered preliminary due to its low sample size. All subjects voluntarily participated in the study after being informed via informed consent.

2.2. The angiosome concept

Angiosome is defined as a specified body area, to which blood flow is governed by a single source artery and thus could be differentiated from adjacent angiosomes (Alexandrescu et al., 2012; Peregrina-Barreto et al., 2014; Khor and Price, 2017). Usually, the lower limb is divided in five to six areas, presented in Fig. 1.

The purple area corresponding to Dorsum Pedis Angiosome (DPA) is supplied by Anterior Tibial Artery. Posterior ankle and anatomical heel are supplied by Posterior Tibial and Peroneal Arteries, forming the Calcaneal Branch (CB, Dark Red) and Posterior Tibial (PA, Green) angiosomes, respectively. Medial Plantar Artery supplies blood to Medial Plantar Angiosome (MPA, Brown). The hallux is occasionally

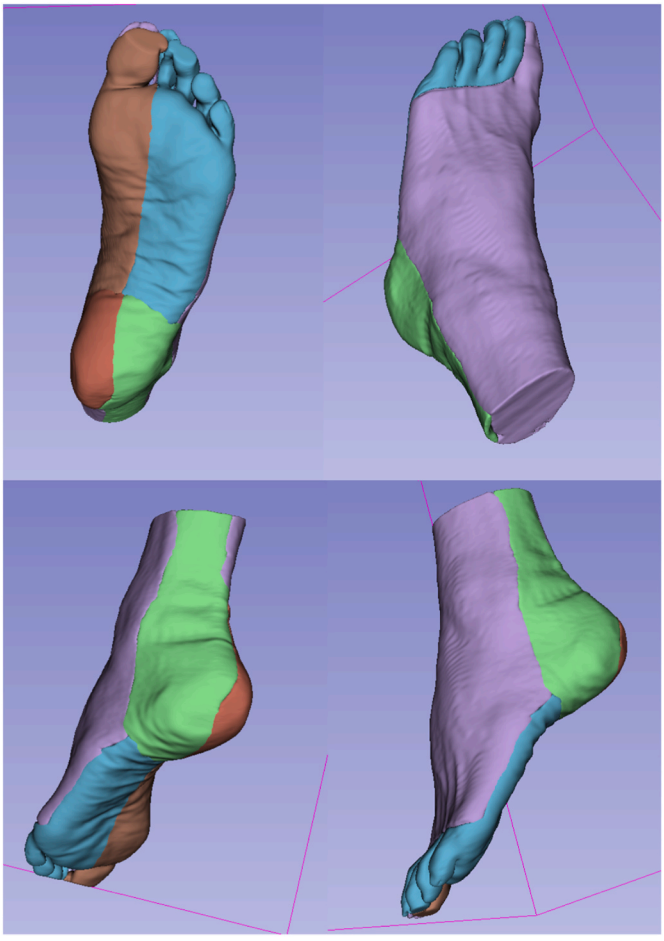

Fig. 1. Lower limb, divided in 5 angiosomes. Illustration of the approximate angiosome locations.

defined as its own angiosome (DML), since both MPA and DPA contribute to its blood flow. The Lateral Plantar Angiosome (LPA, Blue) is supplied by Lateral Plantar Branch.

The angiosome system was first introduced by Taylor and Palmer in 1987 and has been since further conceptualized. (Rother et al., 2015; Seixas et al., 2017; Huang et al., 2015; Sumpio et al., 2013). Angiosomes have been previously studied with diabetes patients (Peregrina-Barreto et al., 2014), for which peripheral arterial diseases and CLTI are part of the clinical status (Nukada, 2014), with ischemic tissue healing due to direct angiosome revascularization (Kabra et al., 2013; Iida et al., 2012) and angiosome specific perfusion abnormalities via radiotracer imaging (Alvelo et al., 2018). The angiosome division could be thought as the source artery mapping on the skin and by establishing the connection between perfusion and heat exchange, one could translate the skin's thermal response to an evaluation of the source artery state.

2.3. Hydrostatic modulation

The hydrostatic modulation test used in this study is a derivation from the Ratschow test, in which the lower limbs are passively elevated and lowered to induce active congestion and ischemia (Pasek et al., 2020; Kawasaki et al., 2013). The advantage of passive limb elevation compared to clinically used cuff modulation methods is avoiding the blocking of the venous circulation. In addition, the cuff-based approach is not accurate for atherosclerotic patients because the cuff pressure must overcome the rigidity of the calcified arterial branch, inducing pain and increased perfusion pressure due to decreased venous return.

In our setup, the hydrostatic modulation is performed by passively elevating the limbs from supine position to an angle θ, measured from the coxae, at the greater trochanter. As an example, the decrease in hydrostatic pressure is approximately $= -g\varrho \int_{h_0}^{h_{elev}} dh = -g\rho l \cdot sin(\theta_{elev})$, where l is the length of the limb. An elevation of 30° from supine position, with $l = 70\ cm$ would correspond to a 27.3 $mmHg$ decrease in hydrostatic pressure, which is in agreement with measurements during lower limb elevation (Wiger and Styf, 1998). The consideration of the hydrostatic component alone though is not completely accurate, since the human body is a dynamical system, i.e. not hydrostatic, and thus there are a number other factors contributing to the final measured pressure difference, such as the orthostatic response and microvascular regulation.

Although the drop in perfusion pressure due to PAD seems to be compensated by the microvascular vasodilation (Anderson et al., 2021; de Graaff and Ubbink, 2003), in case of CLTI, increase in peripheral vascular resistance, drop in SPP and microvascular dysfunction advances to hemodynamic imbalance, where arterial blood pressure and microvascular regulatory function decrease and cell damage occurs. The severity of PAD is also associated with decrease in capillary density that prevents sufficient perfusion and thus oxygen delivery to the tissues, inferior to the occluded artery (Anderson et al., 2021; Signorelli et al., 2020; Anvar et al., 2000). We hypothesize that in case of CLTI, an additional hydrostatic pressure drop Δp cannot be completely compensated due to the increased vascular resistance and decreased blood flow in the main arterial branch, associated with a decreased microvascular function and microvascular density. This could result in overall restricted blood flow and thus, heat delivery within the occluded angiosome.

The decrease in SPP during limb elevation against upright position has been previously demonstrated in a number of studies throughout several decades (Willingham et al., 2016; Rother et al., 2015; Kawasaki et al., 2013; Wiger and Styf, 1998; Beaconsfield and Ginsburg, 1955), yet the total capillary perfusion appears to be regulatorily compensated for healthy individuals during limb elevation against the supine position (Fedorovich et al., 2021). There is no clear consensus if this is the case for CLTI patients.

2.4. Thermal modulation

The thermal modulation tests use either active limb cooling to induce reactive thermal regulation (Lahiri et al., 2020) and thus a rapid thermal recovery, or alternatively active heating (Dremin et al., 2017) of the lower limbs. In this study, thermal cooling was chosen as the thermal modulation method. Based on our pilot measurements, the observed rapid thermal recovery for healthy individuals follows an exponential form (equation (1)) of physical heating with close approximation.

$$T(t) = T_0\ exp(-t/\tau) + A\tau(1 - exp(-t/\tau)) \quad (1)$$

Here T_0 is the initial temperature, A is a scaling constant and τ is the time constant, which is a descriptive metric for thermal recovery rate. The thermal recovery time constant can be solved e.g., by finding least squares fit of Equation (1) for the given temperature recovery recording and by setting A and τ as optimization parameters. Note that Equation (1) serves only as an approximation to the effective thermal recovery behavior of the skin, and thus implies no explanation of the underlying processes. In reality, the active cooling of the limb provokes vasoconstriction (Lahiri et al., 2020), which increases the peripheral vascular resistance and thus, restricts perfusion. After the active cooling period, conduction, convection, and arterial inflow start to heat rapidly the affected tissues provoking vasodilation (Dremin et al., 2017; Liao et al., 2013). Our hypothesis is that for an angiosome governed by an occluded artery, the blood flow and thus the thermal gradient remain smaller during the recovery period, resulting in a significantly higher time constant in Equation (1) or possibly to a poor exponential fit due to the complexity of the compensatory mechanisms. Similar approach has been used previously by Merla et al., in 2000 for cold provocation recovery analysis. However, the connection to current diagnostic parameters, such as ABI and TBI have not been established.

2.5. Test setup and measurement protocol

The test protocol is divided into 5 phases 1) reference data collection 2) Rest phase 3) Limb elevation 4) Hydrostatic recovery and 5) thermal modulation. Completing all test phases, the total execution time is approximately 50 min.

The used test equipment was two FLIR E8 microbolometer thermal cameras with 320 × 240 pixel spatial resolution, 60 mK noise equivalent temperature difference (NETD) and ±2% absolute accuracy from the reading. The data was acquired using the FLIR Tools + software with 9Hz acquisition rate and 0.98 emissivity for skin (Jones and Plassmann, 2002). The reference ABI and TBI measurements were conducted prior the TI with a medical CE certified Viasonix Falcon Pro (Viasonix, Israel) vascular assessment device. The measurements were conducted in a temperature controlled (24.5 °C ± 1.5°C) examination room.

The setup consists of a modified patient bed allowing constant field-of-view (FOV) and relative angle during the modulation tests. A polymethyl methacrylate thermal blocker screen was used to restrict stray infrared radiation (IR) and to aid image processing. The test setup is presented in Fig. 2.

Hydrostatic modulation test was divided in 3 subphases: stabilization (8 min), limb elevation (3 min) and recovery (3 min). In thermal modulation tests, plantar and dorsal lower limbs were simultaneously and symmetrically cooled by moldable cold pads. Alternative cooling methods, such as cold-water submerging (Janský et al., 2003), or cooled air (Das et al., 2016; Kaczmarek and Nowakowski, 2016) were found unsuitable for CLTI patients. The cooling process and conformity was followed periodically with the thermal cameras, until the desired temperature drop had been reached uniformly, i.e. 15% temperature drop from the initial reading (°C) for both limbs, which corresponds approximately to 2.5–5 °C. Fabric cloth insulation was used to avoid

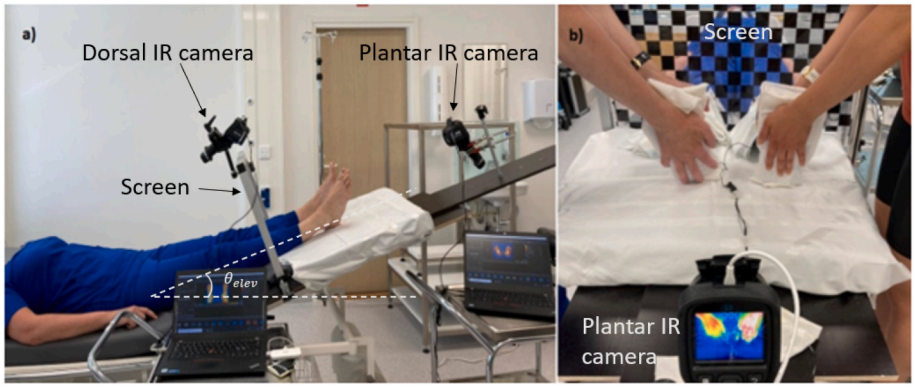

Fig. 2. Test setup from lateral view in the elevated limbs configuration (a) and cold pad thermal modulation (b). The thermal (IR) cameras and the thermal blocker screen are annotated in the figures.

direct skin contact and to moderate the conductivity. The measurement was continued until the asymptotic recovery curve has been reached i.e., the 30 s mean temperature had not increased over 0.5 °C. The recovery period lasted for 10–15 min for each subject.

2.6. Motion correction

Limb movement and slow lower limb drifting was noticeable throughout the measurements for all subjects. Fig. 3 presents limb movement and drifting changes the measurement location.

Small-scale motion artifacts were found detrimental especially in spectral measurements, where low amplitude temperature variations are inspected. Additionally, the ankle extension during hydrostatic modulation changes the plantar and dorsal plane orientation with respect to the camera plane, thus changing the region of interest (ROI) area coverage. To prevent plantar or dorsal feet covering, physical limb fixation was found unsuitable. Additionally, minor movements are difficult to eliminate completely and the ankle extension during hydrostatic elevation is necessary. Thus, computational motion correction was used, where rigid transformations (translation and rotation) were

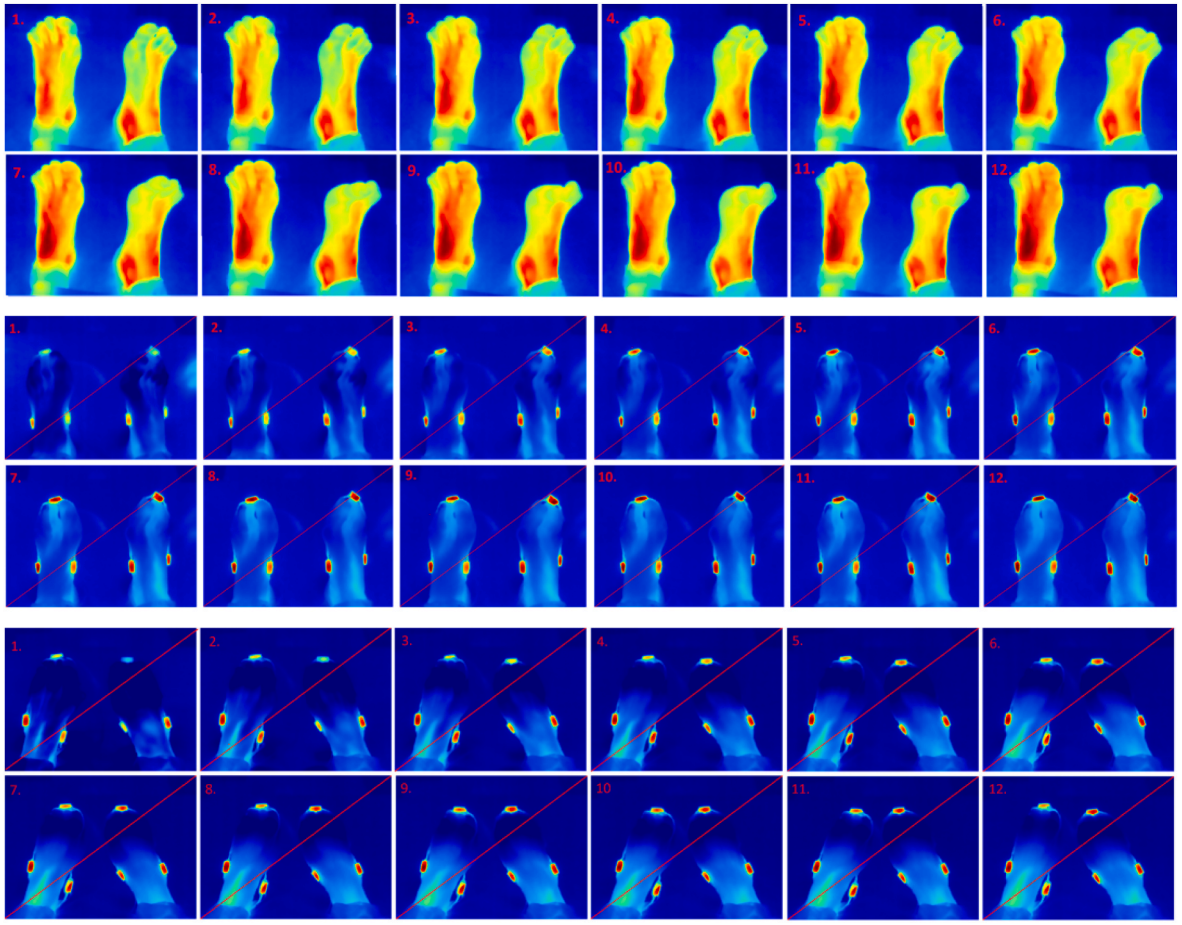

Fig. 3. Timelapse with 1-min intervals from the dorsal camera demonstrating the drifting for three healthy test subjects during the thermal modulation recovery. The drifting is significant especially for the right limb hallux in the 1st series. Slight lateral and medial motion are visible in the 2nd series in relation to the diagonal reference line. The 3rd series presents significant medial inversion drifting.

computed via iterative, intensity based multiresolution optimization. The optimization was performed for every image frame against a reference image (at t_0), and the resulting transformation matrices were used to rotate and translate each respective frame. Maximum bounds were defined for the transformation matrix components according to the expected extent of the limb movement between subsequent frames ($t_i - t_{i-1}$). This eliminates problems caused by the NUC frames and ignores ambiguous frame optimizations results due to divergence. It also results in lesser iteration rounds and thus speeds up the process considerably. In this study, the registration was aided by using low conduction ceramic thermal markers that were attached to the sides of the patient's feet. The markers held a constant temperature slightly above the body temperature and were thus visible in the image frames (Fig. 4). It is important to use sufficient insulation at the attachment boundary to avoid thermal conduction to the skin.

Image resolution and frame rate is preferred to be kept modest due to large number of registration frames. Simple rigid registration, with no scaling or shear appears to be sufficient for rest phase and thermal modulation measurements. We found that either deformative, affine registration or a rigid registration with ROI re-delineation might be used during the elevated period. The latter is preferred, due to the preservation of the original thermography data.

2.7. Measurement parameters and analysis methods

Plantar and dorsal limb datasets were analyzed for each patient by delineating the angiosome ROIs, resulting in 3 datasets on the dorsal side (DPA, LPA and DML) and 5 datasets on the plantar side (MPA, LPA, PA, CB and DML) for both limbs. Additional ROIs were added for possible ulcers and necrotic areas. Each dataset consists of thermal and hydrostatic modulation measurement data, which resulted in 64 measured temperature curves for each subject, and in total 384 time series were computed with methods presented in Table 1. The data was processed and analyzed with Matlab R2020b based, open-source thermal imaging research platform (Pakarinen et al., 2022). All data was resampled and preprocessed prior to the analysis. Motion correction was applied to the resampled data. The analysis parameters for each test phase and the reference measurements are presented in Table 1.

Each parameter is measured as a median value of a region of interest covering a sufficient number of pixels to reduce noise (Budzan and Wyżgolik, 2015). The ROIs are delineated near the center of mass for each angiosome with clear margins to adjacent angiosomes to minimize interference. The setup is used to measure absolute and relative measurements. The latter is performed as contralateral limb analysis, where adjacent limbs for healthy individuals are expected to have similar thermal behavior and properties (Gatt et al., 2015; Vardasca et al., 2012), whereas asymmetric behavior could be expected for PAD and CLTI patients (Nagase et al., 2011).

The thermal recovery data was resampled to 3Hz using 3-frame mean temperature values for each pixel to increase the Signal to Noise Ratio (SNR). The thermal recovery is a relatively slow process containing mainly low spectral frequencies within the endothelial (0.005–0.02 Hz) and DC bands, thus the resulting 1Hz sampling rate is sufficient for determining the time constant in Equation (1). The final recovery curves represent the time dependent, (spatial) median temperature within each angiosome. The time constants (τ) were solved from Equation (1) for each angiosome via least squares function fitting.

Data was excluded from the thermal modulation analysis if the goodness-of-fit (GOF) parameters (GOF R-square under 0.7) or visual inspection of the fit was poor, or if the active cooling temperature drop was less than 1.5 °C for the given area. The hydrostatic modulation data was excluded in cases of unsuccessful registration or large motion artifacts. Finally, the Pearson Rho correlation coefficients against reference metrics were computed using the angiosome mean temperatures. The correlation was determined either as high ($|\rho| \geq 0.70$), high to moderate ($0.70 > |\rho| \geq 0.60$), moderate ($0.60 > |\rho| \geq 0.40$) or low to no correlation ($|\rho| < 0.40$).

3. Results

3.1. Hydrostatic modulation comparison between groups

Table 2 presents the relative mean temperature differences of contralateral angiosomes for the rest, elevated and recovery periods. The table also presents the endothelial and neurogenic spectral powers in each test phase.

The data indicates that the contralateral angiosome differences are lowest for healthy subjects in all hydrostatic test phases and that the hydrostatic modulation has no clear impact on the contralateral difference. The test phase and angiosome specific temperatures are presented in the supplementary material for all CLTI patients and healthy individuals. There is no detectable relation between hydrostatic test phases and mean angiosome temperatures. Hydrostatic mean temperature results for healthy subjects show no specific response or dependence on the hydrostatic test, except that the recovery period temperature is mainly higher than the elevation, yet the temperature decrease or increase between rest and elevation phases seems to follow no pattern.

The endothelial and neurogenic band powers are highest for the healthy individuals in the rest phase, as expected. The elevation and rest phases show band power drop for healthy individuals and PAD patients, yet a higher value for CLTI group. The neurogenic band powers are higher for both PAD and CLTI groups during elevation. Additionally, the contralateral mean band power differences showed high asymmetry (>50%) for all groups.

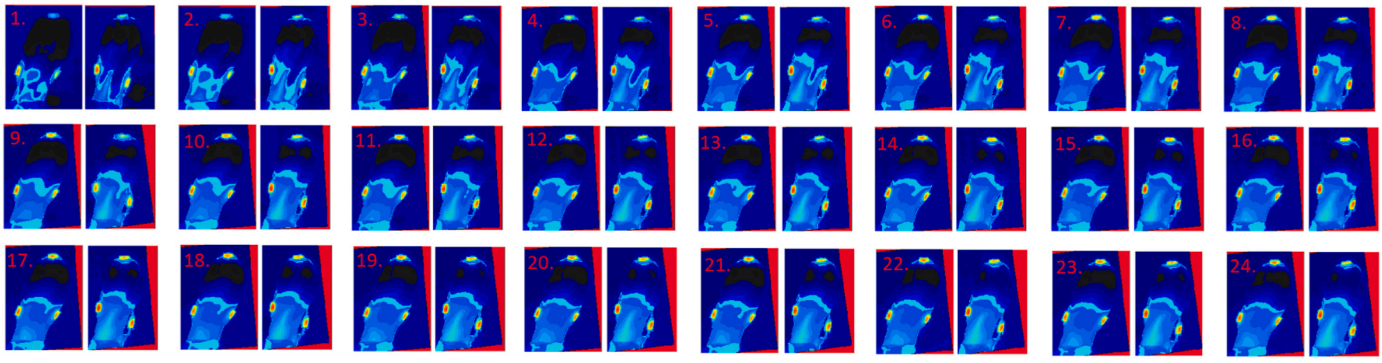

Fig. 4. Low resolution registration time lapse of one test subject illustrating the required rotation and translation correction. The registration is performed for all video frames (targets), against the 1st frame (reference). Here each indexed pair consists of the left limb (left side) and the mirrored right limb (right side). The red background area coverage indicates the required transformation to correct the motion artifacts, such as drifting. The three hot spots located at the limb boundary are thermal markers.

Table 1
Reference and analysis parameters for different test phases.

Reference parameters	ABI, TBI	Age	Diagnosis
Hydrostatic modulation	Angiosome specific temperature differences	Spatial standard deviation to detect locational changes, such as mottling (Ferraris et al., 2018)	Spectral band powers in endothelial and neurogenic temperature fluctuation bands (Geyer et al., 2004; Sagaidachnyi et al., 2016)
Thermal modulation	Thermal recovery (Merla et al., 2000) - time constants and curve shape	Temperature differences (Soliz et al., 2016) between test modulation phases	

Table 2
Mean (std) relative contralateral temperature differences, and relative endothelial (PowE) and neurogenic (PowN) spectral band power differences. ΔPow is the spectral power relative to healthy individuals during the rest phase. The values were measured as the average band powers from all angiosomes free from artifacts.

	Healthy Rest	Healthy Elev	Healthy Recov	PAD Rest	PAD Elev	PAD Recov	CLTI Rest	CLTI Elev	CLTI Recov
ΔT	0.65% (0.2%)	0.57% (0.17%)	0.43% (0.25%)	0.98% (0.23%)	0.99% (0.51%)	0.78% (0.69%)	0.70% (0.38%)	0.80% (0.18%)	0.78% (0.17%)
ΔPowE	100%	73%	50%	63%	44%	51%	65%	96%	57%
ΔPowN	100%	82%	51%	65%	79%	47%	51%	115%	54%

3.2. Thermal modulation comparison between groups

Table 3 presents the mean thermal recovery time constant values and standard deviations for healthy individuals, PAD and CLTI groups.

Table 3 shows that the mean recovery time constants were 88% larger for PAD subjects with claudication and 83% larger for CLTI subjects relative to the healthy young reference. However, the sample size was small and deviation within the groups was high, especially for PAD subjects.

In contralateral limb measurements the lateral symmetry should be high (Gatt et al., 2015; Vardasca et al., 2012) and thus discrepancy in thermal profiles may indicate an underlying vascular condition. Table 4 presents the mean relative differences between the lateral sides for plantar angiosomes and Table 5 for the dorsal angiosomes.

The contralateral limb relative time constant measures in Tables 4–5 show high similarity with healthy young subjects especially in plantar angiosomes, excluding DML. The mean time constant differences relative to maximum were 11% (8% STD) for healthy young subjects, 15% (9% STD) for PAD subjects, and 25% (9% STD) for CLTI subjects. Time constants from function fits with low GOF with poor visual estimate or with no proper cooling (less than 1.5 °C) were excluded. Fig. 5 presents the angiosome specific time constants for 3 healthy individuals.

Both examples show high contralateral symmetry, especially on the plantar angiosomes. Fig. 6 shows time constants for the CLTI patients.

CLTI patient (N = 2) shown in Fig. 6 had a necrotic area on the right limb's 3rd phalanx and a necrotic wound on the 4th phalanx. The left side 5th digit was previously amputated. CLTI patient (N = 3) had a total popliteal artery block on both limbs and necrotic 5th phalanx on the left side. The missing data indicated that the time constant was too large for meaningful comparison or could not be defined for the area. The TBI was used as a reference for patient (N = 3), since ABI could not be defined for the left limb. The right limb ABI was 0.85 (no CLTI).

The contralateral differences in part of the ROIs or in time constants were too large to be comparable i.e., recovery curves did not follow the exponential function or there is no detectable thermal recovery. The necrotic area time constant for the left limb for the CLTI patient (N = 3) could not be defined, since the ROI temperature did not recover. There is an indication of overall lateral asymmetry in thermal recovery time constants in comparison to the healthy individuals.

Table 3
Mean thermal recovery time constants in minutes from all angiosomes.

	Healthy young (N = 3)	PAD with claudication (N = 4)	CLTI (N = 4)
Subject 1	1.52 min	1.91 min	2.68 min
Subject 2	0.86 min	3.94 min	1.55 min
Subject 3	1.19 min	1.94 min	1.84 min
Subject 4		1.19 min	2.65 min
Mean	1.19 min	2.24 min	2.18 min
Standard deviation	0.33 min	1.18 min	0.56 min

Table 4
Mean recovery time constant differences between contralateral plantar angiosomes relative to maximum. (*GOF or minimum cooling requirements not met for any subject for the given angiosome).

	MPA	LPA	PA	CB	DML
Healthy young	0.05	0.06	0.13	0.03	0.45
PAD with claudication	0.15	0.87*	0.26	0.15	0.13
CLTI	0.18	0.38	0.26	0.31	0.30

Table 5
Mean recovery time constant differences between contralateral dorsal angiosomes relative to maximum.

	DPA	LPA	DML
Healthy young	0.19	0.23	0.31
PAD with claudication	0.02	0.17	0.48
CLI	0.14	0.21	0.40

3.3. Thermal imaging and the severity of PAD and CLTI

Thermal recovery time constants are presented in relation to the reference measurements (TBI and ABI) in Fig. 7.

As seen in Fig. 7, thermal recovery time constant has high negative linear correlation with TBI (ρ = *-0.73*). The correlation with ABI is somewhat lower (ρ = *-0.60)*. ABI also shows signs of divergence around the *ABI* = 0.5 - 0.6. Although this could be a result from low sample size, one explanation could relate to the fact that ABI reliability at this range is not clear due to possible media sclerosis, overestimating the measured ankle pressure. The TBI correlations with LPA and DML angiosomes independently were ρ = *-0.71*, ρ = *-0.49,* respectively. The linear fits are presented in the supplementary material in Figures A.7 and A.8. The spatial STD relation to ABI (ρ = *-0.47*) is presented in A.9.

The mean temperatures over all angiosomes, elevation and recovery periods are presented in Fig. 8. No dependency was discovered between temperature and ABI. Also, the hydrostatic intervention by limb elevation did not have a significant effect on the mean temperature. The spatial STD against test phases is presented in A.10.

As seen in Fig. 8 there is no linear correlation with the absolute mean temperatures and ABI and the inter-individual deviation is larger than

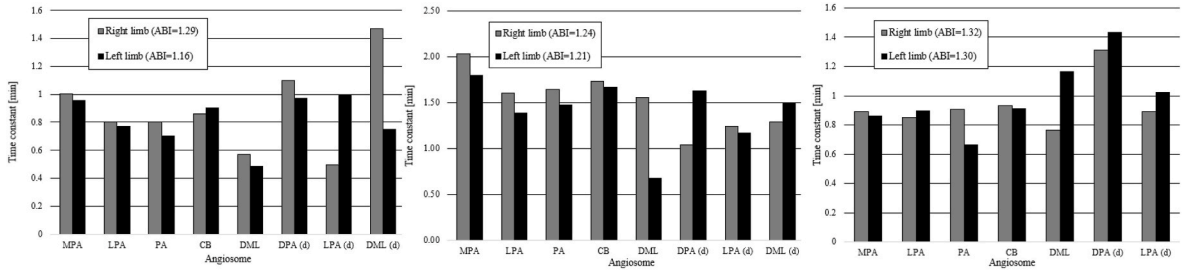

Fig. 5. Angiosome specific contralateral time constants for healthy young subjects. The measured angiosomes were medial and lateral plantar angiosomes (MPA, LPA), posterior tibial angiosome (PA), calcaneal branch (CB), hallux (DML) and dorsum pedis angiosome (DPA). The dorsal angiosomes are indicated with (d).

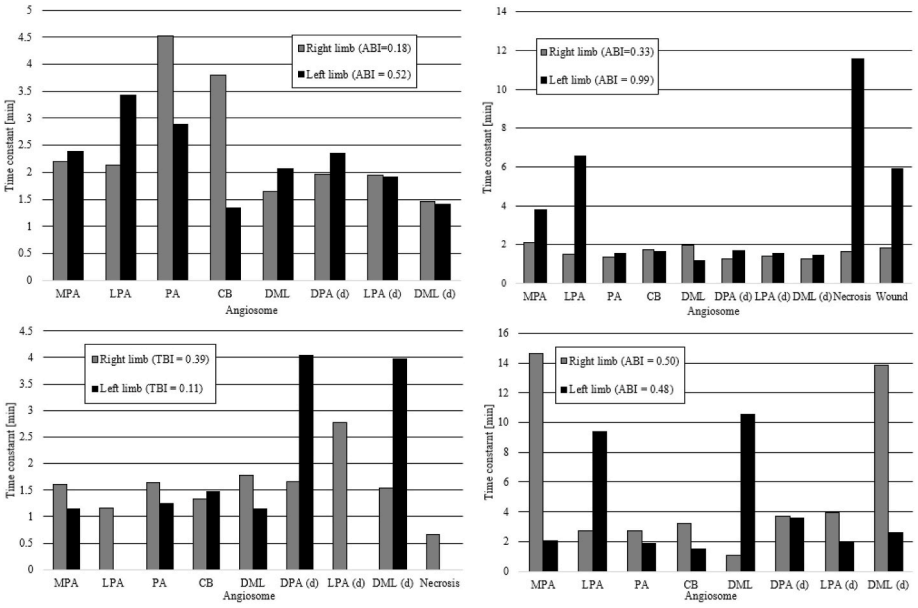

Fig. 6. Angiosome specific contralateral time constants for all CLTI patients. The measured angiosomes were medial and lateral plantar angiosomes (MPA, LPA), posterior tibial angiosome (PA), calcaneal branch (CB), hallux (DML) and dorsum pedis angiosome (DPA). Dorsal angiosomes marked with (d).

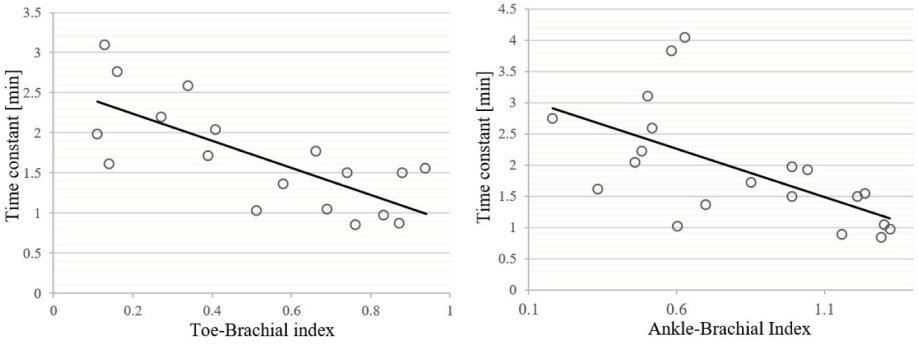

Fig. 7. Thermal modulation recovery time constant from lateral angiosomes (LPA and DML) in relation to TBI and all angiosomes in relation to ABI. TBI shows high negative correlation ($\rho = -0.73$). The relation to ABI shows high to moderate negative correlation ($\rho = -0.60$).

the induced temperature change. Additionally, there is no monotonic correlation calculated with Spearman's correlation ($r_s = 0.044, p = 0.86$). The results for TBI are similar.

Finally, contralateral relative temperature change during hydrostatic test is presented in Fig. 9.

The relative temperature was computed as the mean angiosome temperature difference between rest and elevation, standardized by the maximum test phase temperature (equation (2)).

$$T_{rel} = \frac{T_{rest} - T_{elev}}{max(T_{rest}, T_{elev}, T_{recov})} \quad (2)$$

Fig. 9 shows no correlation with ABI and variation is high. Also, the recovery rate to initial temperature of the cooled limb showed only low negative correlation ($\rho = -0.30$) with ABI, presented in Figure A.11.

Small thermal oscillation spectral band power analysis showed no correlation between reference measurements ABI and band powers (endothelial and neurogenic), with $\rho = 0.23$ and $\rho = 0.15$, respectively.

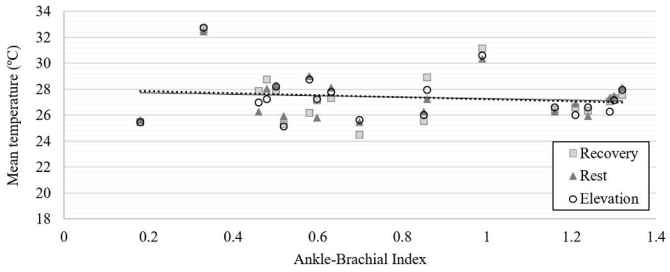

Fig. 8. Mean temperatures in each hydrostatic phase (rest, elevation, recovery). Temperature values show no correlation with ABI with $\rho = -0.11$, $\rho = -0.15$, $\rho = -0.10$, respectively.

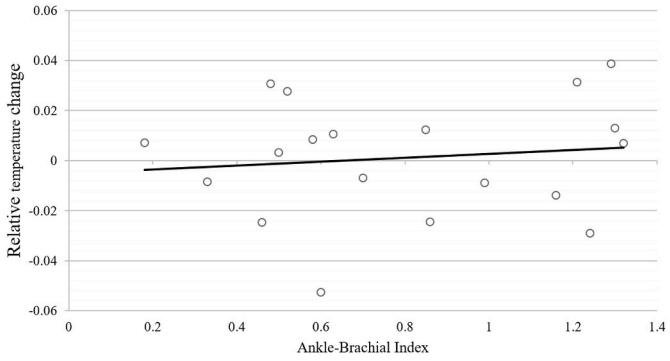

Fig. 9. Relative temperature change between rest and elevation with respect to ABI shows no correlation ($\rho = 0.12$) and high variance.

The linear correlation was slightly higher between TBI and endothelial ($\rho = 0.39$, $R^2 = 0.15$) and neurogenic ($\rho = 0.37$, $R^2 = 0.14$) band powers in steady state. It is worth noting that a 2nd order predictive model could be justified over linear regression due to the 2nd order relation between change in spectral density function and the corresponding band power ($R^2 = 0.22$, $R^2 = 0.19$). The model fits are presented in supplementary material Figure A.12 and A.13.

4. Discussion

This study introduced a thermal imaging test setup for thermal and hydrostatic modulation tests and investigates their feasibility and potential in CLTI diagnostics. Similar approaches have become more common in PAD research due to the technological advances and better affordability for high quality thermal cameras. However, measurement methodology, especially for absolute temperatures (Gatt et al., 2015), measured metrics and their connection to clinical diagnostics are lacking. The peripheral thermal behavior due to arterial occlusion is not completely clear due to multiple coexisting factors, such as several vascular regulatory mechanisms - the regulatory response in different stages of PAD and for CLTI, and the severity and the thermoregulatory effect of microcirculatory dysfunction (Anderson et al., 2021). Additionally, the inter-angiosome artery-to-artery connections contribute to the adjacent angiosome blood flow (Huang et al., 2015). Standardization and reproducibility of thermal measurements are limited by large number of peripheral temperature confounding dependencies within individuals e.g., circadian rhythm, sleep deprivation and light (Cuesta et al., 2017), sex specificity (Martínez-Téllez et al., 2018; Chudecka and Lubkowska, 2015; Vinkers et al., 2013; Kaciuba-Uscilko and Grucza, 2001), acute stress (Vinkers et al., 2013; Herborn et al., 2015), physical activity (Neves et al., 2015), age and body mass index (Lahiri et al., 2020) and other medical conditions affecting on thermoregulation, such as Raynaud's syndrome (Gardner-Medwin et al., 2001; Greenstein et al., 1995). Hence, significance of absolute temperature measures in CLTI diagnostics remains uncertain, and they do not necessarily provide meaningful information alone. In order to eliminate or minimize the confounding factors, the thermal environment should be strictly controlled, including ambient temperature, humidity, airflow, thermal conduction, and thermal radiation (Gagge and Nishi, 2011).

In this study we found a prolonging in thermal recovery time constants for the central angiosomes in CLTI and PAD patients, supporting our initial hypothesis. The high negative correlation of recovery time constant to TBI and ABI implies that even an approximative exponential model of physical heating may be sufficient to evaluate the impaired perfusion and thus, heat delivery. Similar conclusions have been made by Kaczmarek and Nowakowsk in 2016. Part of the thermal recovery results can be explained with the age difference of the compared groups. A research paper from Lahiri et al., in 2020 showed strong positive correlation ($\rho = 0.94$) with cold provocation inversion time and age. However, the recovery time for our preliminary data cannot be completely explained with the subject's age, with moderate positive correlation ($\rho = 0.61$). In future research a healthy age control group will be included for a more in-depth analysis.

The lateral symmetry for angiosome specific mean temperatures and thermal modulation time constant were high for healthy individuals and especially for plantar angiosomes, excluding the DML angiosome. It worth noting that DML is supplied from 2 different arteries, thus being a combination of 2 different angiosomes (MPA and DPA) rather than an individual angiosome, by definition. There was also an indication of contralateral asymmetry for CLTI patients, especially in necrotic areas and ulcers. Thermal images with proper windowing can offer an intuitive visual representation of the regional differences and aid in initial determination of the affected angiosomes. Example thermal profiles are presented in the supplementary material in Figures A.14 - A.16.

The lack of correlation between absolute temperatures and the reference measurements in any hydrostatic test phase questions our initial hypothesis. Only a single healthy subject presented clear response to the modulation, but it is possible that this individual result is a consequence from the microbolometer sensor NUC stabilization, although efforts were made to prevent and to correct baseline and calibration frame artifacts. The results considering the contralateral and inter-individual absolute temperatures conflict with some of the previous studies (Strzelecki et al., 2017; Zenunaj et al., 2021; Gatt et al., 2018). However, the usefulness of absolute temperatures in PAD evaluation has been also questioned previously (Ilo et al., 2020). Carabott et al., in 2021 also found that the hydrostatic elevation did not have significant effect on temperature profiles on PAD patients. This seems to be the case also for CLTI patients.

The relation between reference metrics and the small temperature fluctuations could not be reliably quantified with the current test equipment. Prior studies suggest that thermal cameras with noise equivalent temperature difference of 60 mK (NETD) should be sufficient for endothelial and neurogenic band determination (Sagaidachnyi et al., 2016, 2017), but we must conclude that the thermal cameras used in this study have too low absolute accuracy (±2% from reading) and high NETD ($60mK$) for spectral measurements or in determination of small thermal fluctuations. Hence, proceeding with the data collection for this part with current equipment is not ethically justifiable. The hydrostatic measurements should be repeated using thermal cameras with higher absolute temperature accuracy, lower NETD (preferably NETD $\leq$ 20 mK) and stricter test conditions.

5. Conclusions

In this work we examined the relation between chronic limb threatening ischemia and dynamic thermal imaging, utilizing the angiosome concept, hydrostatic and thermal modulation tests. There is evidence supporting our hypothesis for the thermal time constant prolonging due to severity of PAD and exponential fit validity, yet a difference in absolute temperatures and decreased perfusion due to

hydrostatic modulation could not be confirmed and more research is required with stricter test conditions and larger sample size. Regional asymmetry for CLTI patients, especially for thermal recovery, and moderate symmetry for healthy individual in contralateral analysis advocate the diagnostic potential of relative temperature measures and angiosome division. Measurement of absolute temperatures and small thermal fluctuations require particular attention in standardizing the measurement environment and high camera sensitivity and accuracy. Additionally, the challenges in minimizing motion artefact and patient positioning must be considered carefully, especially for CLTI patients for who facultative immobilization is difficult. We recommend the combination of minimally compulsive fixation to prevent larger motion together with computerized motion correction. The camera framerate should allow multiple frames averaging and angiosome delineation should cover large portion of the angiosomes, so that spatial filtering may be used to increase signal-to-noise ratio. Additionally, estimated angiosome boundaries should be excluded with clear margins to minimize adjacent artery interference. Dynamic thermal imaging has potential as a supportive future technology in CLTI diagnostics, yet its implications and real value are still unclear, though worthy of further research.

Funding sources

This research was funded by the Academy of Finland (351471, 351472), State Research Fund (VTR, 9AP052), and by Instrumentarium Science Foundation, Finland, as a personal grant for Tomppa Pakarinen's doctoral research.

Declaration of competing interest

The authors declare that they have no known competing financial interests or personal relationships that could have appeared to influence the work reported in this paper.

CRediT authorship contribution statement

Tomppa Pakarinen: Conceptualization, Methodology, Software, Formal analysis, Investigation, Data curation, Writing – original draft, Visualization, Funding acquisition. **Atte Joutsen:** Methodology, Investigation, Resources. **Niku Oksala:** Conceptualization, Writing – review & editing, Supervision, Project administration, Resources, Funding acquisition. **Antti Vehkaoja:** Conceptualization, Writing – review & editing, Supervision, Resources, Funding acquisition.

Data availability

The authors do not have permission to share data.

Acknowledgements

Authors have no competing interest to declare. This research was funded by the Academy of Finland (351471, 351472), State Research Fund (VTR, 9AP052), and by Instrumentarium Science Foundation, Finland, as a personal grant for Tomppa Pakarinen's doctoral research. Research nurses Anna-Maija Purosola and Milka Ahola, and medical student Julia Koskela are acknowledged for collecting the preliminary data.

Appendix A. Supplementary data

Supplementary data to this article can be found online at https://doi.org/10.1016/j.jtherbio.2023.103467.

References

Alexandrescu, Vlad, Söderström, M., Venermo, Maarit, 2012. Angiosome theory: fact or fiction? Scand. J. Surg.: SJS: Off. Organ Finnish Surg. Soc. Scandinavian Surg. Soc. 101, 125–131.

Alvelo, J.L., Papademetris, X., Mena-Hurtado, C., Jeon, S., Sumpio, B.E., Sinusas, A.J., Stacy, M.R., 2018. Radiotracer imaging allows for noninvasive detection and quantification of abnormalities in angiosome foot perfusion in diabetic patients with critical limb ischemia and nonhealing wounds. Circulation. Cardiovasc. Imag. 11 (5), e006932 https://doi.org/10.1161/CIRCIMAGING.117.006932.

Anderson, C.P., Pekas, E.J., Park, S.Y., 2021. Microvascular dysfunction in peripheral artery disease: is heat therapy a viable treatment? Mar 1 Int. J. Environ. Res. Publ. Health 18 (5), 2384. https://doi.org/10.3390/ijerph18052384, 33804430; PMCID: PMC7967745.

Anvar, M.D., Khiabani, H.Z., Nesland, J.M., Stranden, E., Kroese, A.J., 2000. Vascular and stromal features in the skin of the lower limb in patients with chronic critical limb ischaemia (CLI) and oedema. Aug Eur. J. Vasc. Endovasc. Surg. 20 (2), 125–131. https://doi.org/10.1053/ejvs.2000.1142. PMID: 10942683.

Bagavathiappan, S., Saravanan, T., Philip, J., Jayakumar, T., Raj, B., Karunanithi, R., Panicker, T.M., Korath, M.P., Jagadeesan, K., 2009. Infrared thermal imaging for detection of peripheral vascular disorders. J. Med. Phys. 34 (1), 43–47. https://doi.org/10.4103/0971-6203.48720.

Bagavathiappan, S., Philip, J., Jayakumar, T., et al., 2010. Correlation between plantar foot temperature and diabetic neuropathy: a case study by using an infrared thermal imaging technique. J. Diabetes Sci. Technol. 4 (6), 1386–1392. https://doi.org/10.1177/193229681000400613.

Beaconsfield, P., Ginsburg, J., 1955. Effect of changes in limb posture on peripheral blood flow. Sep Circ. Res. 3 (5), 478–482. https://doi.org/10.1161/01.res.3.5.478. PMID: 13250716.

Bharara, M., Cobb, J.E., Claremont, D.J., 2006. Thermography and thermometry in the assessment of diabetic neuropathic foot: a case for furthering the role of thermal techniques. Int. J. Low. Extrem. Wounds 5 (4), 250–260. https://doi.org/10.1177/1534734606293481.

Budzan, S., Wyżgolik, R., 2015. Remarks on noise removal in infrared images. Meas. Autom. Monit. 61, 187–190.

Chudecka, M., Lubkowska, A., 2015. Thermal maps of young women and men. Infrared Phys. Technol. 69, 81–87.

Cuesta, M., Boudreau, P., Cermakian, N., Boivin, D.B., 2017. Skin temperature rhythms in humans respond to changes in the timing of sleep and light. Jun J. Biol. Rhythm. 32 (3), 257–273. https://doi.org/10.1177/0748730417702974. Epub 2017 Jun 1. PMID: 28569119.

Das, A., Sarda, A., De, A., 2016. Cooling devices in laser therapy. J. Cutan. Aesthetic Surg. 9 (4), 215–219. https://doi.org/10.4103/0974-2077.197028.

de Graaff, J.C., Ubbink, D.T., van der Spruit, J.A., Lagarde, S.M., Jacobs, M.J., 2003. Influence of peripheral arterial disease on capillary pressure in the foot. Nov J. Vasc. Surg. 38 (5), 1067–1074. https://doi.org/10.1016/s0741-5214(03)00603-7. PMID: 14603219.

Dremin, V.V., Zherebtsov, E.A., Sidorov, V.V., Krupatkin, A.I., Makovik, I.N., Zherebtsova, A.I., Zharkikh, E.V., Potapova, E.V., Dunaev, A.V., Doronin, A.A., Bykov, A.V., Rafailov, I.E., Litvinova, K.S., Sokolovski, S.G., Rafailov, E.U., 2017. Multimodal optical measurement for study of lower limb tissue viability in patients with diabetes mellitus. Aug J. Biomed. Opt. 22 (8), 1–10. https://doi.org/10.1117/1.JBO.22.8.085003. PMID: 28825287.

Fedorovich, A.A., Loktionova, Y.I., Zharkikh, E.V., Mikhailova, M.A., Popova, J.A., Suvorov, A.V., Zherebtsov, E.A., 2021. Body position affects capillary blood flow regulation measured with wearable blood flow sensors. Diagnostics 11 (3), 436. https://doi.org/10.3390/diagnostics11030436.

Ferraris, A., Bouisse, C., Mottard, N., Thiollière, F., Anselin, S., Piriou, V., Allaouchiche, B., 2018. Mottling score and skin temperature in septic shock: relation and impact on prognosis in ICU. PLoS One 13 (8), e0202329. https://doi.org/10.1371/journal.pone.0202329.

Gagge, A.P., Nishi, Y., 2011. Heat exchange between human skin surface and thermal environment. Compr. Physiol. https://doi.org/10.1002/cphy.cp090105.

Gardner-Medwin, J.M., Macdonald, I.A., Taylor, J.Y., Riley, P.H., Powell, R.J., 2001. Seasonal differences in finger skin temperature and microvascular blood flow in healthy men and women are exaggerated in women with primary Raynaud's phenomenon. Jul Br. J. Clin. Pharmacol. 52 (1), 17–23. https://doi.org/10.1046/j.0306-5251.2001.01405.x. PMID: 11453886; PMCID: PMC2014513.

Gatt, A., Formosa, C., Cassar, K., Camilleri, K.P., De Raffaele, C., Mizzi, A., Azzopardi, C., Mizzi, S., Falzon, O., Cristina, S., Chockalingam, N., 2015. Thermographic patterns of the upper and lower limbs: baseline data. Int. J. Vasc. Med. 2015, 831369 https://doi.org/10.1155/2015/831369.

Gatt, Alfred, Falzon, Owen, Cassar, Kevin, Ellul, Christian, Camilleri, Kenneth, Gauci, Jean, Mizzi, Stephen, Mizzi, Anabelle, Delia, Sturgeon, Cassandra, Camilleri, Liberato, Chockalingam, Nachiappan, Formosa, Cynthia, 2018. Establishing differences in thermographic patterns between the various complications in diabetic foot disease. Int. J. Endocrinol. 2018, 1–7. https://doi.org/10.1155/2018/9808295.

Gerhard-Herman, M., et al., 2017. 2016 AHA/ACC guideline on the management of patients with lower extremity peripheral artery disease. Circulation 135, e686–e725.

Geyer, M., Yih-Kuen, J., Brienza, D., Boninger, M., 2004. Using wavelet analysis to characterize the thermoregulatory mechanisms of sacral skin blood flow. J. Rehabil. Res. Dev. 41, 797–806. https://doi.org/10.1682/JRRD.2003.10.0159.

Greenstein, D., Gupta, N.K., Martin, P., Walker, D.R., Kester, R.C., 1995. Impaired thermoregulation in Raynaud's phenomenon. Jul Angiology 46 (7), 603–611. https://doi.org/10.1177/000331979504600707. PMID: 7618763.

Herborn, K.A., Graves, J.L., Jerem, P., et al., 2015. Skin temperature reveals the intensity of acute stress. Physiol. Behav. 152 (Pt A), 225–230. https://doi.org/10.1016/j.physbeh.2015.09.032.

Huang, T.Y., Huang, T.S., Wang, Y.C., Huang, P.F., Yu, H.C., Yeh, C.H., 2015. Direct revascularization with the angiosome concept for lower limb ischemia: a systematic review and meta-analysis. Aug Medicine (Baltim.) 94 (34), e1427. https://doi.org/10.1097/MD.0000000000001427. PMID: 26313796; PMCID: PMC4602934.

Iida, O., Soga, Y., Hirano, K., Kawasaki, D., Suzuki, K., Miyashita, Y., Terashi, H., Uematsu, M., 2012. Long-term results of direct and indirect endovascular revascularization based on the angiosome concept in patients with critical limb ischemia presenting with isolated below-the-knee lesions. J. Vasc. Surg. 55 (2), 363–370. https://doi.org/10.1016/j.jvs.2011.08.014 e5.

Ilo, A., Romsi, P., Mäkelä, J., 2020. Infrared thermography as a diagnostic tool for peripheral artery disease. Adv. Skin Wound Care 33 (9), 482–488. https://doi.org/10.1097/01.ASW.0000694156.62834.8b.

Janský, L., Vávra, V., Janský, P., Kunc, P., Knižková, I., Jandová, D., Slováček, K., 2003. Skin temperature changes in humans induced by local peripheral cooling. J. Therm. Biol. 28 (5), 429–437. https://doi.org/10.1016/s0306-4565(03)00028-7.

Jones, B.F., Plassmann, P., 2002. Digital infrared thermal imaging of human skin. IEEE Eng. Med. Biol. Mag. 21 (6), 41–48. https://doi.org/10.1109/MEMB.2002.1175137. Nov.-Dec.

Kabra, A., Suresh, K.R., Vivekanand, V., Vishnu, M., Sumanth, R., Nekkanti, M., 2013. Outcomes of angiosome and non-angiosome targeted revascularization in critical lower limb ischemia. J. Vasc. Surg. 57 (1), 44–49. https://doi.org/10.1016/j.jvs.2012.07.042.

Kaciuba-Uscilko, H., Grucza, R., 2001. Gender differences in thermoregulation. Nov Curr. Opin. Clin. Nutr. Metab. Care 4 (6), 533–536. https://doi.org/10.1097/00075197-200111000-00012. PMID: 11706289.

Kaczmarek, Mariusz, Nowakowski, Antoni, 2016. Active IR-thermal imaging in medicine. J. Nondestr. Eval. 35 https://doi.org/10.1007/s10921-016-0335-y.

Kawasaki, T., Uemura, T., Matsuo, K., Masumoto, K., Harada, Y., Chuman, T., Murata, T., 2013. The effect of different positions on lower limbs skin perfusion pressure. Sep Indian J. Plast. Surg. 46 (3), 508–512. https://doi.org/10.4103/0970-0358.121995. PMID: 24459340; PMCID: PMC3897095.

Khor, B., Price, P., 2017. The comparative efficacy of angiosome-directed and indirect revascularisation strategies to aid healing of chronic foot wounds in patients with co-morbid diabetes mellitus and critical limb ischaemia: a literature review. J. Foot Ankle Res. 10, 26.

Lahiri, B.B., Bagavathiappan, S., Philip, J., 2020. Infrared thermal imaging based study of localized cold stress induced thermoregulation in lower limbs: the role of age on the inversion time. Dec J. Therm. Biol. 94, 102781. https://doi.org/10.1016/j.jtherbio.2020.102781. Epub 2020 Nov 14, PMID: 33292979.

Liao, F., Burns, S., Jan, Y.K., 2013. Skin blood flow dynamics and its role in pressure ulcers. J. Tissue Viability 22 (2), 25–36. https://doi.org/10.1016/j.jtv.2013.03.001.

Mambou, S.J., Maresova, P., Krejcar, O., Selamat, A., Kuca, K., 2018. Breast cancer detection using infrared thermal imaging and a deep learning model. Sensors 18 (9), 2799. https://doi.org/10.3390/s18092799.

Martínez-Téllez, Borja, Ortiz, Alvarez, Lourdes, Sánchez-Delgado, Guillermo, Xu, Huiwen, Acosta, Francisco, Ramírez, Merchán, Elisa, Hernández, Victoria, Martínez-Avila, Wendy, Contreras-Gomez, Miguel, Gil, Ángel, Labayen, Idoia, Ruiz, Jonatan, 2018. Skin temperature response to a liquid meal intake is different in men than in women. Clin. Nutr. 38 https://doi.org/10.1016/j.clnu.2018.05.026.

Merla, Arcangelo, Donato, L., Romani, Gian-Luca, 2000. Tau Image: a Diagnostic Imaging Technique Based on the Dynamicdigital Telethermography, vol. 2, pp. 1223–1226. https://doi.org/10.1109/IEMBS.2000.897951 vol. 2.

Misra, S., Shishehbor, M.H., Takahashi, E.A., Aronow, H.D., Brewster, L.P., Bunte, M.C., Kim, E.S.H., Lindner, J.R., Rich, K., 2019. American heart association council on peripheral vascular disease; council on clinical cardiology; and council on cardiovascular and stroke nursing. Perfusion assessment in critical limb ischemia: principles for understanding and the development of evidence and evaluation of devices: a scientific statement from the American heart association. Sep 17 Circulation 140 (12), e657–e672. https://doi.org/10.1161/CIR.0000000000000708. Epub 2019 Aug 12. PMID: 31401843; PMCID: PMC7372288.

Mori, T., Nagase, T., Takehara, K., Oe, M., Ohashi, Y., Amemiya, A., Noguchi, H., Ueki, K., Kadowaki, T., Sanada, H., 2013. Morphological pattern classification system for plantar thermography of patients with diabetes. J. Diabetes Sci. Technol. 7 (5), 1102–1112. https://doi.org/10.1177/193229681300700502.

Nagase, T., Sanada, H., Takehara, K., Oe, M., Iizaka, S., Ohashi, Y., Oba, M., Kadowaki, T., Nakagami, G., 2011. Variations of plantar thermographic patterns in normal controls and non-ulcer diabetic patients: novel classification using angiosome concept. Jul J. Plast. Reconstr. Aesthetic Surg. 64 (7), 860–866. https://doi.org/10.1016/j.bjps.2010.12.003. Epub 2011 Jan 22. PMID: 21257357.

Neves, E., Vilaça-Alves, J., Antunes, N., Felisberto, I., Rosa, C., Reis, V., 2015. Different responses of the skin temperature to physical exercise: systematic review. In: 2015 37th Annual International Conference of the IEEE Engineering in Medicine and Biology Society. EMBC), pp. 1307–1310. https://doi.org/10.1109/EMBC.2015.7318608.

Nukada, Hitoshi, 2014. Ischemia and diabetic neuropathy. Handb. Clin. Neurol. 126, 469–487.

Pakarinen, Tomppa, Oksala, Niku, Vehkaoja, Antti, 2022. IRlab - platform for thermal video analysis in evaluation of peripheral thermal behavior and blood perfusion. Inform. Med. Unlocked 30, 100940. https://doi.org/10.1016/j.imu.2022.100940.

Pasek, Jarosław, Stanek, Agata, Cieslar, Grzegorz, 2020. The role of physical activity in prevention and treatment of peripheral vascular disorders. Acta Angiol. 26, 19–27. https://doi.org/10.5603/AA.2020.0003.

Peregrina-Barreto, H., Morales-Hernandez, L.A., Rangel-Magdaleno, J.J., Avina-Cervantes, J.G., RamirezCortes, J.M., Morales-Caporal, R., 2014. Quantitative estimation of temperature variations in plantar angiosomes: a study case for diabetic foot. Comput. Math. Methods Med. 2014, 585306 https://doi.org/10.1155/2014/585306.

Ring, E.F., Ammer, K., 2012. Infrared thermal imaging in medicine. Physiol. Meas. 33 (3), R33–R46. https://doi.org/10.1088/0967-3334/33/3/R33.

Rother, U., Kapust, J., Lang, W., Horch, R.E., Gefeller, O., Meyer, A., 2015. The angiosome concept evaluated on the basis of microperfusion in critical limb ischemia patients-an oxygen to see guided study. Nov Microcirculation 22 (8), 737–743. https://doi.org/10.1111/micc.12249. PMID: 26399939.

Sagaidachnyi, Andrey, Fomin, A., Skripal, Anatoly, Usanov, D., 2016. Spectral Filtering Approach to the Skin Blood Flow Imaging in Limbs via Infrared Thermography: its Scope and Limits. https://doi.org/10.21611/qirt.2016.109.

Sagaidachnyi, Andrey, Fomin, A., Usanov, D., Skripal, Anatoly, 2017. Thermography-based blood flow imaging in human skin of the hands and feet: a spectral filtering approach. Physiol. Meas. 38, 272–288.

Seixas A., Ammer K., Carvalho R., Vilas-Boas J.P., Vardasca R., Mendes J.. Skin temperature in diabetic foot patients: a study focusing on the angiosome concept. In: Tavares J, Natal Jorge R, editors. VipIMAGE 2017. ECCOMAS. Lecture notes in computational vision and biomechanics, vol. 27. Cham: Springer; 2018. https://doi.org/10.1007/978-3-319-68195-5_114.

Signorelli, S.S., Vanella, L., Abraham, N.G., Scuto, S., Marino, E., Rocic, P., 2020. Pathophysiology of chronic peripheral ischemia: new perspectives. Therapeut. Adv. Chron. Dis. 11, 204062231989446 https://doi.org/10.1177/2040622319894466.

Soliz, P., et al., 2016. Detection of diabetic peripheral neuropathy using spatial-temporal analysis in infrared videos. In: 50th Asilomar Conference on Signals, Systems and Computers, 2016, pp. 263–267. https://doi.org/10.1109/ACSSC.2016.7869038.

Staffa, E., Bernard, V., Kubicek, L., Vlachovsky, R., Vlk, D., Mornstein, V., Staffa, R., 2017. Infrared thermography as option for evaluating the treatment effect of percutaneous transluminal angioplasty by patients with peripheral arterial disease. Vascular 25 (1), 42–49.

Strzelecki, Michal, Strakowska, Maria, Strąkowski, Robert, Kaszuba, A., 2017. Cold provocation and active thermography in medical screening. Comput. Methods Sci. Technol. 23, 65–71. https://doi.org/10.12921/cmst.2017.0000007.

Sumpio, B.E., Forsythe, R.O., Ziegler, K.R., van Baal, Lepantalo, M.J., Hinchliffe, R.J., 2013. Clinical implications of the angiosome model in peripheral vascular disease. J. Vasc. Surg. 58 (3), 814–826. https://doi.org/10.1016/j.jvs.2013.06.056.

Tehan, P.E., Santos, D., Chuter, V.H., 2016. A systematic review of the sensitivity and specificity of the toe-brachial index for detecting peripheral artery disease. Vasc. Med. 21 (4), 382–389. https://doi.org/10.1177/1358863X16645854.

Vardasca, Ricardo, Ring, E.F.J., Plassmann, P., Jones, Carl, 2012. Termal symmetry of the upper and lower extremities in healthy subjects. Thermol. Int. 22, 53–60.

Vinkers, C.H., Penning, R., Hellhammer, J., Verster, J.C., Klaessens, J.H., Olivier, B., Kalkman, C.J., 2013. The effect of stress on core and peripheral body temperature in humans. Sep Stress 16 (5), 520–530. https://doi.org/10.3109/10253890.2013.807243. Epub 2013 Jul 9. PMID: 23790072.

Wiger, P., Styf, J.R., 1998. Effects of limb elevation on abnormally increased intramuscular pressure, blood perfusion pressure, and foot sensation: an experimental study in humans. J. Orthop. Trauma 12 (5), 343–347. https://doi.org/10.1097/00005131-199806000-00008. Jun-Jul, PMID: 9671186.

Willingham, T.B., Southern, W.M., McCully, K.K., 2016. Measuring reactive hyperemia in the lower limb using near-infrared spectroscopy. Sep J. Biomed. Opt. 21 (9), 091302. https://doi.org/10.1117/1.JBO.21.9.091302. PMID: 27050534.

Xu, Dachun, Li, Jue, Zou, Liling, Xu, Yawei, Hu, Dayi, Pagoto, S.L., Ma, Yunsheng, 2010. Sensitivity and specificity of the ankle–brachial index to diagnose peripheral artery disease: a structured review. Vasc. Med. 15 (5), 361–369. https://doi.org/10.1177/1358863X10378376.

Zenunaj, G., Lamberti, N., Manfredini, F., Traina, L., Acciarri, P., Bisogno, F., Scian, S., Serra, R., Abatangelo, G., Gasbarro, V., 2021. Infrared thermography as a diagnostic tool for the assessment of patients with symptomatic peripheral arterial disease undergoing infrafemoral endovascular revascularisations. Sep 17 Diagnostics 11 (9), 1701. https://doi.org/10.3390/diagnostics11091701. PMID: 34574042; PMCID: PMC8469591.